

Three-Dimensional Fermi Surface of Overdoped La-Based Cuprates

M. Horio,¹ K. Hauser,¹ Y. Sassa,² Z. Mingazheva,¹ D. Sutter,¹ K. Kramer,¹ A. Cook,¹ E. Nocerino,³ O. K. Forslund,³ O. Tjernberg,³ M. Kobayashi,⁴ A. Chikina,⁴ N. B. M. Schröter,⁴ J. A. Krieger,^{5,6} T. Schmitt,⁴ V. N. Strocov,⁴ S. Pyon,⁷ T. Takayama,⁷ H. Takagi,⁷ O. J. Lipscombe,⁸ S. M. Hayden,⁸ M. Ishikado,⁹ H. Eisaki,¹⁰ T. Neupert,¹ M. Måansson,³ C. E. Matt,^{1,4,11} and J. Chang¹

¹Physik-Institut, Universität Zürich, Winterthurerstrasse 190, CH-8057 Zürich, Switzerland

²Department of Physics and Astronomy, Uppsala University, SE-75121 Uppsala, Sweden

³Department of Applied Physics, KTH Royal Institute of Technology, Electrum 229, SE-16440 Stockholm Kista, Sweden

⁴Swiss Light Source, Paul Scherrer Institut, CH-5232 Villigen PSI, Switzerland

⁵Laboratory for Muon Spin Spectroscopy, Paul Scherrer Institute, CH-5232 Villigen PSI, Switzerland

⁶Laboratorium für Festkörperphysik, ETH Zürich, CH-8093 Zürich, Switzerland

⁷Department of Advanced Materials, University of Tokyo, Kashiwa 277-8561, Japan

⁸H. H. Wills Physics Laboratory, University of Bristol, Bristol BS8 1TL, United Kingdom

⁹Comprehensive Research Organization for Science and Society (CROSS), Tokai, Ibaraki 319-1106, Japan

¹⁰Electronics and Photonics Research Institute, National Institute of Advanced Industrial Science and Technology, Ibaraki 305-8568, Japan

¹¹Department of Physics, Harvard University, Cambridge, MA 02138, USA.

We present a soft x-ray angle-resolved photoemission spectroscopy study of overdoped high-temperature superconductors. In-plane and out-of-plane components of the Fermi surface are mapped by varying the photoemission angle and the incident photon energy. No k_z dispersion is observed along the nodal direction, whereas a significant antinodal k_z dispersion is identified for La-based cuprates. Based on a tight-binding parametrization, we discuss the implications for the density of states near the van-Hove singularity. Our results suggest that the large electronic specific heat found in overdoped $\text{La}_{2-x}\text{Sr}_x\text{CuO}_4$ can not be assigned to the van-Hove singularity alone. We therefore propose quantum criticality induced by a collapsing pseudogap phase as a plausible explanation for observed enhancement of electronic specific heat.

The nature of the pseudogap phase in high-temperature cuprate superconductors remains an outstanding problem [1]. It has at the same time been associated with different types of broken symmetries [2–6] and interpreted as a crossover phenomenon with an ill-defined temperature onset [7]. In recent years, a connection between the pseudogap collapse as a function of doping and the Fermi level (E_F) crossing of the van-Hove singularity (VHS) has been proposed [8–11]. In this scenario, the pseudogap exists only on a hole-like Fermi surface (FS) sheet. In particular, for the La-based cuprates, it was suggested that the pseudogap phase is truncated at the doping where the VHS crosses E_F [12]. This coincides approximately with a maximum in the electronic specific heat peaks [13, 14]. Therefore electronic specific heat enhancement could be a signature of quantum criticality due to the vanishing pseudogap phase at the doping $p = p^*$. Or, it could be explained simply from density-of-states (DOS) enhancement generated by the VHS. The latter scenario is expected to be significant for quasi-two-dimensional band structures [15]. Experimentally, it has thus become important to determine the out-of-plane FS structure of La-based cuprates.

Quantum oscillation (QO) and angle-resolved photoemission spectroscopy (ARPES) experiments are classical probes of the FS structure and quasi-particle renormalization effects [16, 17]. Both techniques have been applied to overdoped $\text{Ti}_2\text{Ba}_2\text{CuO}_{6+\delta}$ (Tl2201) compounds

for which a single large FS sheet is observed [18–21]. The observation of a single QO frequency suggests that if any k_z dependence exists, it is weak. In contrast, angle-dependent magneto-transport experiment has been interpreted as an evidence of a finite FS k_z dispersions [22]. To date, ARPES has not provided any information about three dimensionality of the FS in the cuprates. The vast majority of ARPES experiments have been carried out in the vacuum-ultra-violet regime [16]. For 20–200 eV photons, the photoelectron mean free path (MFP) is a few Å [23], resulting in considerable k_z broadening [23]. Only few ARPES studies of cuprate superconductors exist in the soft x-ray regime [24–27], where much larger MFP and thus better k_z resolution is reached. Soft x-ray ARPES (SX-ARPES) has been applied to $\text{YBa}_2\text{Cu}_3\text{O}_{7-\delta}$ [26] to reach bulk sensitivity and overcome the polar catastrophe [28]. In $\text{La}_{2-x}\text{Sr}_x\text{CuO}_4$ (LSCO), the $d_{3z^2-r^2}$ band has been probed by use of distinctive photoionization matrix elements in the soft x-ray regime [27]. To date, however, there are no reports on FS k_z dispersion for La-based cuprates. Such information is especially desirable since the connection between VHS and pseudogap is most relevant for these compounds [9].

Here, we apply SX-ARPES to reveal the FS k_z dispersion of three different cuprates, namely, LSCO ($x = 0.22$), $\text{La}_{1.8-x}\text{Eu}_{0.2}\text{Sr}_x\text{CuO}_4$ (Eu-LSCO, $x = 0.21$), and Tl2201. The first mentioned compound does not display any pseudogap physics (i.e. $p > p^*$), and hence

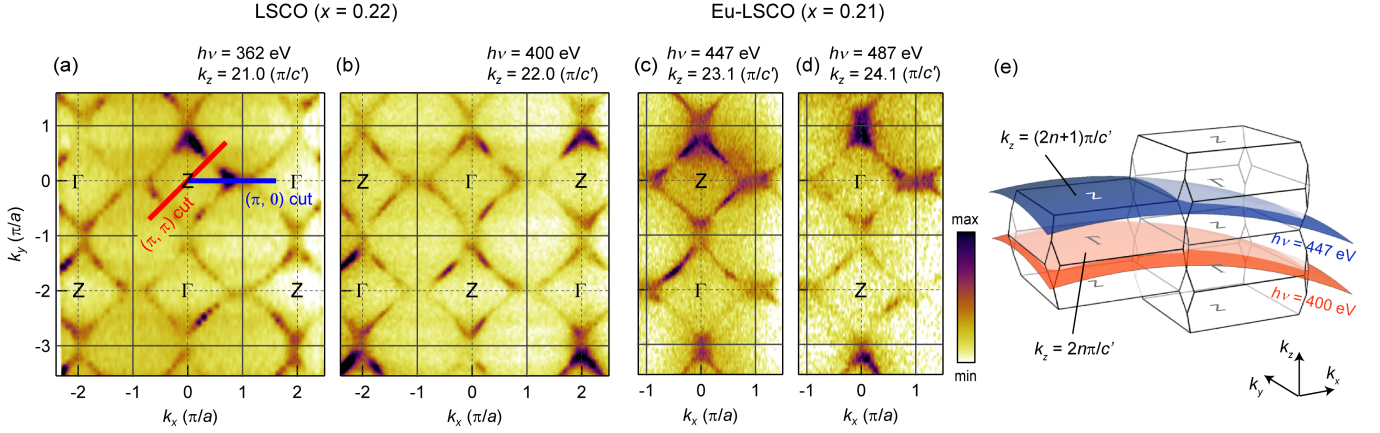


FIG. 1. In-plane FSs of LSCO ($x = 0.22$) (a),(b) and Eu-LSCO ($x = 0.21$) (c),(d) measured at $T = 12$ K using SX-ARPES. Photoelectron intensities have been integrated ± 20 meV around E_F . Corresponding k_z value at $(k_x, k_y) = (0, 0)$ is indicated on the right top of each panel along with the associated incident photon energies. (e) Sketch of the Brillouin zone and location of the in-plane cuts in the 3D momentum space at $\hbar\nu = 400$ and 447 eV.

the FS is well defined. Secondly, this specific composition of LSCO has body-centered tetragonal (BCT) crystal structure, and therefore, orthorhombic band folding is avoided [29, 30]. No discernible k_z dependence is found along the nodal direction. By contrast, a clear k_z dependence is found in the antinodal region for the La-based cuprates. This dispersion is parametrized using a single-band tight-binding model. Including inter-layer hopping t_z to reproduce the observed band structure, the corresponding DOS is not large enough to explain the specific heat anomaly. Our results suggest that the VHS alone cannot account for the specific-heat enhancement, and therefore support the scenario that associates quantum criticality arising from the collapse of the pseudogap phase.

Single crystals of LSCO ($x = 0.22$, $T_c = 22$ K), Eu-LSCO ($x = 0.21$, $T_c = 15$ K), and Tl2201 ($T_c = 20$ K) were grown by the floating-zone and self-flux techniques. Crystal lattice parameters a and c are listed in Table I. The sample quality has been demonstrated previously by experiments [31–35] on the same batch of crystals. Experiments were carried out at the SX-ARPES end-station [36] of the ADRESS beamline [37] at the Swiss Light Source (SLS) of the Paul Scherrer Institute (PSI), Switzerland. ARPES spectra were recorded at $T = 12$ K with 300–600 eV circularly polarized photons covering more than three Brillouin zones in both in- and out-of-plane directions. The energy and momentum resolution depend on the exact incident photon energy. For 500 eV photons, the effective resolution is ~ 90 meV and $\sim 0.02 \pi/a$ for energy and momentum, respectively (full width at half maximum). Measurements were carried out with the analyzer slit oriented parallel to the incident x rays as in Ref. 36. Pristine surfaces were realized using a top post or a cleaving tool [38]. To

index high-symmetry points in three-dimensional reciprocal space (k_x, k_y, k_z) , we use the BCT notation with $\Gamma = (0, 0, 0)$, $Z = (0, 0, \pi/c')$, $\Sigma = ([1 + \eta]\pi/a, 0, 0)$, and $\Sigma_1 = ([1 - \eta]\pi/a, 0, \pi/c')$, where $c' = c/2$ represents CuO₂-layer spacing and $\eta = a^2/4c'^2$. The out-of-plane momentum is given by

$$\hbar k_z = \sqrt{2m[(\hbar\nu - \phi - E_B) \cos^2(\theta) + V_0]} + p_c \sin \alpha \quad (1)$$

where m is the electron mass, ϕ the work function, E_B the binding energy, θ the photoemission polar angle, V_0 the inner potential, \hbar the reduced Planck constant, and p_c is the incident photon momentum that is significant for SX-ARPES. The incident grazing angle α was set to 20° . For the inner potential, we assumed $V_0 = 15$ eV consistent with what has been used for pnictide materials [39, 40]. For our density-functional-theory (DFT) calculations, the WIEN2k package [41] was used.

Maps of the electron-like [34, 42–44] FS topology of LSCO ($x = 0.22$) and Eu-LSCO ($x = 0.21$) for different values of k_z are shown in Fig. 1. Even though k_z varies across these maps [Fig. 1(e)], strong matrix-element effects complicate the extraction of any k_z dispersion. It is therefore better examined by FS-mapping directly along the k_z direction over a wide momentum region. In Figs. 2(a)–(d), nodal (π, π) and antinodal $(\pi, 0)$ cuts as a function of k_z (incident photon energy) are shown. In the nodal direction, no discernible dispersion is observed across two different Brillouin zones. Intensity variations are again assigned to matrix element effects. Along the antinodal direction, by contrast, a clear dispersion of k_F is found. The two FS branches separated by the zone boundary disperse π -shifted along the k_z direction [Figs. 2(b) and (d)]. This π -shift is a direct consequence of the BCT crystal structure where the Γ and the Z points alternate in the in-plane direction [Fig. 2(g)]. As a ref-

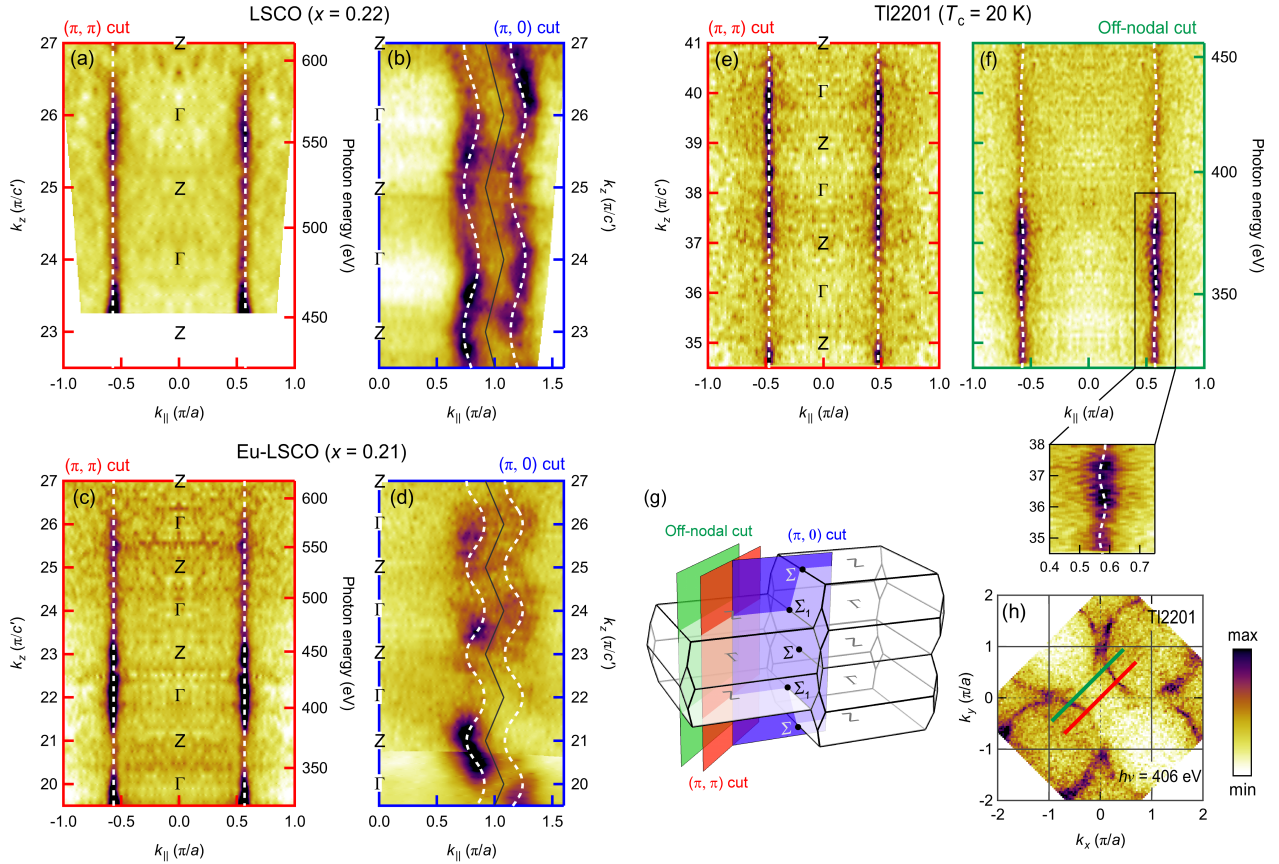


FIG. 2. Out-of-plane FS dispersions. (a)–(d) Out-of-plane FS maps recorded along nodal (π, π) and the antinodal $(\pi, 0)$ directions – as indicated in (g) – for LSCO ($x = 0.22$) and Eu-LSCO ($x = 0.21$). (e),(f) k_z dependence of nodal and off-nodal [see (g) and (h)] k'_F s on the FS of Tl2201. A zoom on the off-nodal k_z dispersion is provided in (f). Nodal out-of-plane maps and data in panels (b) and (f) are symmetrized around $k_{||} = 0$. FSs reproduced by the three-dimensional tight-binding model (see text) are overlaid as white dashed curves. Photoelectron intensities are integrated ± 20 meV around E_F . Black lines in panels (b) and (d) represent Brillouin zone boundaries. (g) Sketch of the three-dimensional Brillouin zone and location of the cuts. (h) In-plane FS map of Tl2201 with nodal (π, π) and off-nodal cuts indicated.

erence, nodal and off-nodal k_z dispersions of the more two-dimensional Tl2201 system are shown in Figs. 2(e) and (f).

To parametrize the three-dimensional FS structure, we use a simple tight-binding model decomposed into two terms: $\epsilon_{3D}(k_x, k_y, k_z) = \epsilon_{2D}(k_x, k_y) + \epsilon_z(k_x, k_y, k_z)$. Although band structure of La-based cuprates involves hybridization of $d_{x^2-y^2}$ and $d_{3z^2-r^2}$ orbitals [27], we – for simplicity – employ an effective single band ($d_{x^2-y^2}$) model:

$$\begin{aligned} \epsilon_{2D}(k_x, k_y) &= -\mu + 2t[\cos(k_x a) + \cos(k_y a)] \\ &+ 4t' \cos(k_x a) \cos(k_y a) + 2t'' [\cos(2k_x a) + \cos(2k_y a)], \end{aligned} \quad (2)$$

where t , t' , and t'' represent first-, second-, and third-nearest-neighbor hopping parameters, and μ is the chemical potential. The out-of-plane dispersion reads:

$$\epsilon_z(k_x, k_y, k_z) = 2t_z \sigma [\cos(k_x a) - \cos(k_y a)]^2 \cos(k_z c') \quad (3)$$

where t_z denotes an inter-layer hopping parameter [15]. The term $[\cos(k_x a) - \cos(k_y a)]$ arises from the hybridization between O 2p and Cu 4s or $3d_{3z^2-r^2}$ orbitals that promote hopping along the c -axis [45, 46]. A characteristic of the BCT structure is that it has an offset of successive CuO₂ planes in the diagonal in-plane direction by $(a/2, a/2)$, generating an additional factor $\sigma = \cos(k_x a/2) \cos(k_y a/2)$ [15]. The out-of-plane FS of LSCO ($x = 0.22$) was fitted to this tight-binding model (Fig. 2). The obtained in-plane hopping parameters (see Table I) are consistent with the previous studies [43, 47]. From the k_z antinodal dispersion, we in addition extract the out-of-plane hopping parameter t_z . For both LSCO ($x = 0.22$) and Eu-LSCO ($x = 0.21$), fitting with Eq. 3 provided a good description of the observed dispersion with $t_z = 0.07t$. In overdoped La-based cuprates, t_z/t thus constitutes a significant fraction. For comparison, overdoped Tl2201, with a hole-like in-plane FS, yields a

	LSCO ($x = 0.22$)	Eu-LSCO ($x = 0.21$)	Tl2201 ($T_c = 20$ K)
$a = b$	3.76 Å	3.79 Å	3.87 Å
$c = 2c'$	13.22 Å	13.14 Å	23.20 Å
t'	-0.12 t	-0.14 t	-0.28 t
t''	0.06 t	0.07 t	0.14 t
μ	0.93 t	0.95 t	1.44 t
t_z	0.07 t	0.07 t	($<$) 0.015 t

TABLE I. Lattice constants and parameters for three-dimensional tight-binding model. $c' = c/2$ represents CuO₂-layer spacing. Tight-binding parameters are expressed as a fraction of the nearest-neighbor hopping parameter t . A fixed ratio $t'' = -0.5t'$ has been assumed [43].

k_z dispersion [see Fig. 2(f)] with $t_z/t < 0.015$.

We start our discussion by pointing to a known discrepancy in overdoped LSCO, between bulk hole doping and the FS area [34, 43]. The tight-binding extracted FS area, equivalent to $p = 0.32$ and 0.31 for LSCO ($x = 0.22$) and Eu-LSCO ($x = 0.21$), is significantly larger than the nominal Sr concentrations. A stronger k_z dependence in the overdoped region had been put forward as an explanation [43]. Having measured the three-dimensional FS, this scenario is eliminated. It has also been hypothesized that the cleaved surface may have a higher doping than the bulk. Our SX-ARPES is more bulk sensitive and should thus alleviate the discrepancy. As this is not the case, this scenario is also not plausible. The filling of overdoped La-based cuprates thus remains puzzling but has no qualitative impact on the following discussion.

Having quantified the out-of-plane hopping, it is interesting to discuss transport anisotropy ratios. Sr₂RuO₄ and overdoped LSCO are isostructural and both display low-temperature Fermi liquid behavior [48, 49]. The ratio ρ_c/ρ_{ab} between out-of-plane (ρ_c) and in-plane (ρ_{ab}) resistivity is about 100 for LSCO [48, 50] and 1000 for Sr₂RuO₄ [49] which even has a shorter c -axis lattice parameter ($c = 12.74$ Å). For overdoped La_{1.6-x}Nd_{0.4}Sr_xCuO₄ (Nd-LSCO), right at the pseudogap critical doping concentration $p^* = 0.24$, an anisotropy factor $\rho_c/\rho_{ab} \sim 200$ is found [51, 52]. These values for La-based cuprates are considerably smaller than what has been found in Tl2201 ($\rho_c/\rho_{ab} \sim 1000\text{--}2500$) [53, 54]. This is consistent with first-principle DFT calculations that predict $t_z/t = 0.12$ for LSCO [15] and 0.01 for Tl2201. For LSCO, this value of t_z is 1.7 times larger than what is found by our experiment. Assuming for 300–600 eV photons a probing depth of 10 Å, the experimental k_z broadening amounts to $\sim 0.2\pi/c'$. The k_z resolution, therefore, does not lead to any significant underestimation of t_z . The discrepancy between experiment and DFT calculations is thus significant. This DFT overestimation of t_z is linked to the $d_{3z^2-r^2}$ orbital that influences

interlayer hopping. DFT places the $d_{3z^2-r^2}$ band closer to E_F than observed experimentally in LSCO [27]. Once the $d_{3z^2-r^2}$ band is far from E_F as in Tl2201 [55], DFT predicts a k_z dispersion consistent with the experiment.

From the antinodal FS k_z dispersion of LSCO and Eu-LSCO, the DOS anomaly generated by the VHS can be estimated. For a given binding energy ω , the two-dimensional DOS(ω) = $\frac{a^2}{2\pi^2} \frac{dA}{d\omega}$ where A is the constant-energy-surface area. The in-plane nearest-neighbor hopping parameter $t = -0.19$ eV is set by the observed nodal Fermi velocity [34, 42, 56]. Averaging along the k_z axis yields the DOS(E_F) versus doping (filling), Fig. 3(a), for (i) a two-dimension FS and (ii) the experimentally determined three-dimensional FS. The divergent peak in the 2D-model is replaced by a plateau once k_z dispersion is introduced. The plateau indicates the doping range for which the FS character (electron- or hole-like) changes as a function of k_z . Crystal symmetry imposes two VHS points (separating electron- and hole-like FSs) to exist at E_F between the Σ and the Σ_1 points. Irrespective of the splitting along k_z of these VHS points, the DOS remains constant because of the fixed number of singularities. The plateau width and height are primarily set by $\bar{t}_z = t_z/t$ and $1/\bar{t}_z$, respectively. In-plane hopping parameters t'/t and t''/t are less important and experimentally known to vary little with doping [43]. Due to the weak doping dependence of lattice parameters, we thus assumed all hopping parameters to be constants [15].

The DOS is proportional to the electronic specific heat (Sommerfeld) coefficient $\gamma = \frac{\pi^2}{3} k_B^2 \times \text{DOS}(E_F)$ and hence directly comparable to measurements of Zn-LSCO [13], LSCO ($x = 0.33$) [48], Eu-LSCO, and Nd-LSCO [14] [see Figs. 3(a) and (b)]. Taking into account the observed k_z dispersion yields a Sommerfeld constant around the VHS that is 0.5–0.7 of the experimental value [13, 48]. Including disorder in our evaluation of DOS only enhance the discrepancy [Fig. 3(c)] because finite quasi-particle lifetime τ suppresses the VHS. For Zn-LSCO (Eu-LSCO and Nd-LSCO), a scattering rate of $\hbar/\tau = 0.28t$ (0.04 t) is expected [14, 57, 58]. In this case the simulated γ peak accounts for less than half of the measured value. Therefore, the VHS alone cannot account for the strong enhancement of the specific heat near $p = p^*$. This implies that sources going beyond band structure are required to explain the specific heat of overdoped LSCO. Quantum criticality originating from the collapse of the pseudogap phase is thus a tangible explanation for the electronic specific heat enhancement.

In summary, we have revealed the full three dimensional FS structure of overdoped La-based cuprates using the SX-ARPES technique. A significant k_z dispersion was observed on the antinodal FS portion while the nodal part of the FS is non-dispersive. The three-dimensional FS was parametrized using the single-band

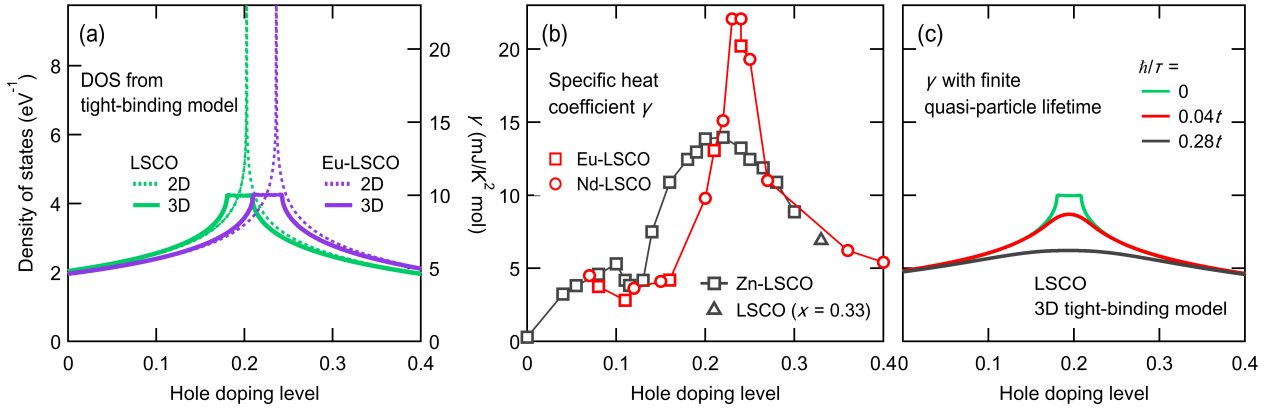


FIG. 3. Comparison of calculated DOS with experimentally extracted Sommerfeld constant γ . (a) Doping dependence of DOS at E_F calculated for LSCO and Eu-LSCO from a tight-binding model (see text and Table I) with $t_z = 0.07t$ (3D) and 0 (2D). The diverging peak in two-dimensions is replaced by a plateau in the three-dimensional model. The right axis indicates the electronic specific heat coefficient $\gamma = \frac{\pi^2}{3} k_B^2 \times \text{DOS}(E_F)$. (b) Doping dependence of γ reported on Zn-LSCO [13], LSCO ($x = 0.33$) [48], Eu-LSCO, and Nd-LSCO [14] plotted on the same scale as in (a). (c) γ values calculated from the 3D tight-binding model for LSCO with quasi-particle scattering rates as indicated.

tight-binding model. In this manner, the out-of-plane hopping term is quantified. Finally, it was shown that the three-dimensional FS structure cannot account for the large electronic specific heat observed in overdoped LSCO. Quantum criticality emerging from the pseudogap collapse provides a plausible explanation for the specific heat anomaly.

We acknowledge fruitful discussions with L. Taillefer, S. Verret, and A.-M. S. Tremblay. M.H., D.S., K.K., J.A.K., and J.C. acknowledge support by the Swiss National Science Foundation (grant numbers: CRSII2_160765, PP00P2_150573, BSSGI0_155873, and 200021_165910). Y.S. and E.N. are funded by the Swedish Research Council (VR) with a Starting Grant (Dnr. 2017-05078) and the Swedish Foundation for Strategic Research (SSF) within the Swedish national graduate school in neutron scattering (SwedNess). O.K.F. and M.M. are supported by Marie Skłodowska-Curie Action, International Career Grant through the European Commission and Swedish Research Council (VR), Grant No. INCA-2014-6426, the Carl Tryggers Foundation for Scientific Research (CTS-16:324), and a VR neutron project grant (BIFROST, Dnr. 2016-06955). T. N. acknowledges support from the Swiss National Science Foundation (grant number: 200021_169061) and from the European Union's Horizon 2020 research and innovation program (ERC-StG-Neupert-757867-PARATOP). The present work was partially supported by JSPS KAKENHI Grant Number JP15K17712. This work was also supported by the Knut and Alice Wallenberg foundation. Sample characterizations on Ti2201 were performed by using SQUID magnetometer (MPMS, Quantum Design Inc.) at the CROSS user laboratories. ARPES measurements were performed

at the ADRESS beamline of the Swiss Light Source at the Paul Scherrer Institute.

-
- [1] M. R. Norman, D. Pines, and C. Kallin, *Advances in Physics* **54**, 715 (2005).
 - [2] L. Zhao, C. A. Belvin, R. Liang, D. A. Bonn, W. N. Hardy, N. P. Armitage, and D. Hsieh, *Nat Phys* **13**, 250 (2017).
 - [3] B. Fauqué, Y. Sidis, V. Hinkov, S. Pailhès, C. T. Lin, X. Chaud, and P. Bourges, *Phys. Rev. Lett.* **96**, 197001 (2006).
 - [4] R. Daou, J. Chang, D. LeBoeuf, O. Cyr-Choinière, F. Laliberté, N. Doiron-Leyraud, B. J. Ramshaw, R. Liang, D. A. Bonn, W. N. Hardy, and L. Taillefer, *Nature* **463**, 519 (2010).
 - [5] M. Hashimoto, R.-H. He, K. Tanaka, J.-P. Testaud, W. Meevasana, R. G. Moore, D. Lu, H. Yao, Y. Yoshida, H. Eisaki, et al., *Nat Phys* **6**, 414 (2010).
 - [6] J. Xia, E. Schemm, G. Deutscher, S. A. Kivelson, D. A. Bonn, W. N. Hardy, R. Liang, W. Siemons, G. Koster, M. M. Fejer, and A. Kapitulnik, *Phys. Rev. Lett.* **100**, 127002 (2008).
 - [7] G. V. M. Williams, J. L. Tallon, and J. W. Loram, *Phys. Rev. B* **58**, 15053 (1998).
 - [8] S. Benhabib, A. Sacuto, M. Civelli, I. Paul, M. Cazayous, Y. Gallais, M.-A. Méasson, R. D. Zhong, J. Schneeloch, G. D. Gu, et al., *Phys. Rev. Lett.* **114**, 147001 (2015).
 - [9] N. Doiron-Leyraud, O. Cyr-Choinière, S. Badoux, A. Ataei, C. Collignon, A. Gourgout, S. Dufour-Beauséjour, F. F. Tafti, F. Laliberté, M. E. Boulanger, et al., *Nat. Commun.* **8**, 2044 (2017).
 - [10] R. S. Markiewicz, I. G. Buda, P. Mistark, C. Lane, and A. Bansil, *Sci. Rep.* **7**, 44008 (2017).
 - [11] W. Wu, M. S. Scheurer, S. Chatterjee, S. Sachdev, A. Georges, and M. Ferrero, *Phys. Rev. X* **8**, 021048

- (2018).
- [12] O. Cyr-Choinière, R. Daou, F. Laliberté, C. Collignon, S. Badoux, D. LeBoeuf, J. Chang, B. J. Ramshaw, D. A. Bonn, W. N. Hardy, et al., *Phys. Rev. B* **97**, 064502 (2018).
 - [13] N. Momono, M. Ido, T. Nakano, M. Oda, Y. Okajima, and K. Yamaya, *Physica C* **233**, 395 (1994).
 - [14] B. Michon, C. Girod, S. Badoux, J. Kamark, M. D. Q. Ma, H. A. Dabkowska, B. D. Gaulin, J.-S. Zhou, S. Pyon, T. Takayama, et al., [arXiv:1804.08502](https://arxiv.org/abs/1804.08502).
 - [15] R. S. Markiewicz, S. Sahrakorpi, M. Lindroos, H. Lin, and A. Bansil, *Phys. Rev. B* **72**, 054519 (2005).
 - [16] A. Damascelli, Z. Hussain, and Z.-X. Shen, *Rev. Mod. Phys.* **75**, 473 (2003).
 - [17] S. E. Sebastian and C. Proust, *Annu. Rev. Condens. Matter Phys.* **6**, 411 (2015).
 - [18] M. Platé, J. D. F. Mottershead, I. S. Elfimov, D. C. Peets, R. Liang, D. A. Bonn, W. N. Hardy, S. Chiuzbian, M. Falub, M. Shi, et al., *Phys. Rev. Lett.* **95**, 077001 (2005).
 - [19] D. C. Peets, J. D. F. Mottershead, B. Wu, I. S. Elfimov, R. Liang, W. N. Hardy, D. A. Bonn, M. Raudsepp, N. J. C. Ingle, and A. Damascelli, *New J. Phys.* **9**, 28 (2007).
 - [20] P. M. C. Rourke, A. F. Bangura, T. M. Benseman, M. Matusiak, J. R. Cooper, A. Carrington, and N. E. Hussey, *New J. Phys.* **12**, 105009 (2010).
 - [21] B. Vignolle, A. Carrington, R. A. Cooper, M. M. J. French, A. P. Mackenzie, C. Jaudet, D. Vignolles, C. Proust, and N. E. Hussey, *Nature* **455**, 952 (2008).
 - [22] N. E. Hussey, M. Abdel-Jawad, A. Carrington, A. P. Mackenzie, and L. Balicas, *Nature* **425**, 814 (2003).
 - [23] V. Strocov, *J. Electron Spectrosc. Relat. Phenom.* **130**, 65 (2003).
 - [24] T. Claesson, M. Måansson, C. Dallera, F. Venturini, C. D. Nadaï, N. B. Brookes, and O. Tjernberg, *Phys. Rev. Lett.* **93**, 136402 (2004).
 - [25] T. Claesson, M. Måansson, A. Önsten, M. Shi, Y. Sassa, S. Pailhés, J. Chang, A. Bendounan, L. Patthey, J. Mesot, et al., *Phys. Rev. B* **80**, 094503 (2009).
 - [26] V. B. Zabolotnyy, A. A. Kordyuk, D. Evtushinsky, V. N. Strocov, L. Patthey, T. Schmitt, D. Haug, C. T. Lin, V. Hinkov, B. Keimer, et al., *Phys. Rev. B* **85**, 064507 (2012).
 - [27] C. E. Matt, D. Sutter, A. M. Cook, Y. Sassa, M. Måansson, O. Tjernberg, L. Das, M. Horio, D. Destraz, C. G. Fatuzzo, et al., *Nat. Commun.* **9**, 972 (2018).
 - [28] N. Nakagawa, H. Y. Hwang, and D. A. Muller, *Nat. Mater.* **5**, 204 (2006).
 - [29] J. Chang, Y. Sassa, S. Guerrero, M. Mnsson, M. Shi, S. Pailhs, A. Bendounan, R. Mottl, T. Claesson, O. Tjernberg, et al., *New J. Phys.* **10**, 103016 (2008).
 - [30] P. D. C. King, J. A. Rosen, W. Meevasana, A. Tamai, E. Rozbicki, R. Comin, G. Levy, D. Fournier, Y. Yoshida, H. Eisaki, et al., *106*, 127005 (2011).
 - [31] O. J. Lipscombe, S. M. Hayden, B. Vignolle, D. F. McMorrow, and T. G. Perring, *Phys. Rev. Lett.* **99**, 067002 (2007).
 - [32] J. Chang, J. S. White, M. Laver, C. J. Bowell, S. P. Brown, A. T. Holmes, L. Maechler, S. Strässle, R. Gilard, S. Gerber, et al., *Phys. Rev. B* **85**, 134520 (2012).
 - [33] C. G. Fatuzzo, Y. Sassa, M. Måansson, S. Pailhès, O. J. Lipscombe, S. M. Hayden, L. Patthey, M. Shi, M. Grioni, H. M. Rønnow, et al., *Phys. Rev. B* **89**, 205104 (2014).
 - [34] J. Chang, M. Måansson, S. Pailhès, T. Claesson, O. J. Lipscombe, S. M. Hayden, L. Patthey, O. Tjernberg, and J. Mesot, *Nat. Commun.* **4**, 2559 (2013).
 - [35] C. E. Matt, C. G. Fatuzzo, Y. Sassa, M. Måansson, S. Fatale, V. Bitetta, X. Shi, S. Pailhès, M. H. Berntsen, T. Kurosawa, et al., *Phys. Rev. B* **92**, 134524 (2015).
 - [36] V. N. Strocov, X. Wang, M. Shi, M. Kobayashi, J. Krempasky, C. Hess, T. Schmitt, and L. Patthey, *J. Synchrotron Rad.* **21**, 32 (2014).
 - [37] V. N. Strocov, T. Schmitt, U. Flechsig, T. Schmidt, A. Imhof, Q. Chen, J. Raabe, R. Betemps, D. Zimoch, J. Krempasky, et al., *J. Synchrotron Rad.* **17**, 631 (2010).
 - [38] M. Måansson, T. Claesson, U. O. Karlsson, O. Tjernberg, S. Pailhès, J. Chang, J. Mesot, M. Shi, L. Patthey, N. Momono, et al., *Rev. Sci. Instrum.* **78**, 076103 (2007).
 - [39] Y.-M. Xu, Y.-B. Huang, X.-Y. Cui, E. Razzoli, M. Radovic, M. Shi, G.-F. Chen, P. Zheng, N.-L. Wang, C.-L. Zhang, et al., *Nat Phys* **7**, 198 (2011).
 - [40] P. Vilmercati, A. Fedorov, I. Vobornik, U. Manju, G. Panaccione, A. Goldoni, A. S. Sefat, M. A. McGuire, B. C. Sales, R. Jin, et al., *Phys. Rev. B* **79**, 220503 (2009).
 - [41] P. Blaha, K. Schwarz, G. Madsen, D. Kvasnicka, and J. Luitz, Wien2k: An Augmented Plane Wave + Local Orbitals Program for Calculating Crystal Properties (Vienna University of Technology, Vienna, 2001) (2001).
 - [42] T. Yoshida, X. J. Zhou, D. H. Lu, S. Komiya, Y. Ando, H. Eisaki, T. Kakeshita, S. Uchida, Z. Hussain, Z.-X. Shen, and A. Fujimori, *J. Phys. Condens. Matter.* **19**, 125209 (2007).
 - [43] T. Yoshida, X. J. Zhou, K. Tanaka, W. L. Yang, Z. Hussain, Z.-X. Shen, A. Fujimori, S. Sahrakorpi, M. Lindroos, R. S. Markiewicz, et al., *Phys. Rev. B* **74**, 224510 (2006).
 - [44] E. Razzoli, Y. Sassa, G. Drachuck, M. Mnsson, A. Keren, M. Shay, M. H. Berntsen, O. Tjernberg, M. Radovic, J. Chang, et al., *New J. Phys.* **12**, 125003 (2010).
 - [45] O. Andersen, A. Liechtenstein, O. Jepsen, and F. Paulsen, *J. Phys. Chem. Solids* **56**, 1573 (1995).
 - [46] T. Xiang and J. M. Wheatley, *Phys. Rev. Lett.* **77**, 4632 (1996).
 - [47] M. Hashimoto, T. Yoshida, H. Yagi, M. Takizawa, A. Fujimori, M. Kubota, K. Ono, K. Tanaka, D. H. Lu, Z.-X. Shen, S. Ono, and Y. Ando, *Phys. Rev. B* **77**, 094516 (2008).
 - [48] S. Nakamae, K. Behnia, N. Mangkorntong, M. Nohara, H. Takagi, S. J. C. Yates, and N. E. Hussey, *Phys. Rev. B* **68**, 100502 (2003).
 - [49] N. E. Hussey, A. P. Mackenzie, J. R. Cooper, Y. Maeno, S. Nishizaki, and T. Fujita, *Phys. Rev. B* **57**, 5505 (1998).
 - [50] Y. Nakamura and S. Uchida, *Phys. Rev. B* **47**, 8369 (1993).
 - [51] R. Daou, N. Doiron-Leyraud, D. LeBoeuf, S. Y. Li, F. Laliberté, O. Cyr-Choinière, Y. J. Jo, L. Balicas, J. Q. Yan, J. S. Zhou, et al., *Nat. Phys.* **5**, 31 (2009).
 - [52] O. Cyr-Choinière, R. Daou, J. Chang, F. Laliberté, N. Doiron-Leyraud, D. LeBoeuf, Y. Jo, L. Balicas, J. Q. Yan, J.-G. Cheng, et al., *Physica C* **470**, S12 (2010).
 - [53] N. E. Hussey, J. R. Cooper, J. M. Wheatley, I. R. Fisher, A. Carrington, A. P. Mackenzie, C. T. Lin, and O. Milat, *Phys. Rev. Lett.* **76**, 122 (1996).
 - [54] H.-J. Kim, P. Chowdhury, S. K. Gupta, N. H. Dan, and S.-I. Lee, *Phys. Rev. B* **70**, 144510 (2004).

- [55] H. Sakakibara, H. Usui, K. Kuroki, R. Arita, and H. Aoki, [Phys. Rev. Lett.](#) **105**, 057003 (2010).
- [56] X. J. Zhou, T. Yoshida, A. Lanzara, P. V. Bogdanov, S. A. Kellar, K. M. Shen, W. L. Yang, F. Ronning, T. Sasagawa, T. Kakeshita, *et al.*, [Nature](#) **423**, 398 (2003).
- [57] T. Yoshida, S. Komiya, X. J. Zhou, K. Tanaka, A. Fujimori, Z. Hussain, Z.-X. Shen, Y. Ando, H. Eisaki, and S. Uchida, [Phys. Rev. B](#) **80**, 245113 (2009).
- [58] S. Verret, O. Simard, M. Charlebois, D. Sénechal, and A.-M. S. Tremblay, [Phys. Rev. B](#) **96**, 125139 (2017).